The impact of input signal deformation on atan2 angle calculation error

Mitja Alič

Faculty of Electrical Enginering, University of Ljubljana, Tržaška cesta 25, 1000 Ljubljana
E-mail: mitja1357@gmail.com

In position sensing encoders and resolvers are used, whose output is a pair of quadrature sine and cosine signals. Angle calculation can be done with atan2 function. Due to improper installation of sensor, sine and cosine signal can be deformed. In that case calculated angle includes error. Error was analyzed for non-equal amplitudes, non-orthogonality, DC offset and common mode signal. Error was analyzed in frequency specter, that yielded a function of error based on input signal deformation. Error is presented in Fourier series form.

1 Introduction

These days the need for high quality motor regulation is present in numerous applications and has as a result become unavoidable. For a consistent and reliable measurement of rotation, position sensors are used [1], such as encoders and resolvers [2][3][4]. Because the output of such sensors is a pair of quadrature sine and cosine signals, angle must first be calculated. The easiest way of doing so is by directly calculating atan2, which returns a value between $[-\pi, \pi]$.

Because position sensors are not ideal, obtained sine and cosine signal can be deformed, phase shifted and DC offset. All of these imperfections cause the calculated angle to also include error.

Literature [5], [6], [7] and [8] analyses the impact of such imperfection for lower harmonics only and states that error of imperfections scale linearly. During our research we found, that the error specter also contains higher harmonics. The paper examines error waveform dependent on input signal mismatch with Fourier analysis.

2 Methodology and results

Output from a position sensor can be represented with

$$Sin = B_0 + B_1 \sin(\theta + \varphi_s) + CMM \quad (1)$$
$$Cos = A_0 + A_1 \cos(\theta + \varphi_c) + CMM \quad (2)$$

Where B_0 and A_0 represent DC offset, B_1 and A_1 signal amplitude, φ_s and φ_c phase shift and θ reference angle. Signals (1) and (2) can also have a common superimposed AC signal represented as CMM (3). CMM can be of cosine or sine form with Δ_c and Δ_s as amplitude.

$$CMM = \Delta_c \cos(\theta) + \Delta_s \sin(\theta) \quad (3)$$

By calculating atan2 for eq. (1) and (2)

$$\varphi = \text{atan2}(Sin, Cos) \quad (4)$$

and then subtracting it with an unaltered signal

$$\varepsilon = \varphi - \text{atan2}(\sin(\theta), \cos(\theta)) \quad (5)$$

we get error based on deformation. Because AC signal analysis is simpler in frequency domain, error was converted with Fast Fourier Transform(FFT). By varying each parameter individually we examined the impact of the parameter in question on specter of error. Output of atan2 was examined by sending each parameter in eq. (1) and (2) to infinity or worst case with phase shift. In this case amplitude and phase of each harmonic approaches to a limit value.

The course of the amplitude and phase in dependence on the changing parameter was approximated by a function, that best suited numerical waveform obtained from the error spectrum. The set of functions decreases by checking the limit value to which each amplitude and phase approach. We were looking for the best approximation with polynomials, rational functions, exponential, trigonometric and cyclometric functions. The best approximation was sought using the minimum squares method.

2.1 Defining of error at different amplitudes

In the first case was observed the impact of different amplitudes on error. The output of the atan2 function is determined by the eq. (1) and (2) quotient. Since only the ratio of the amplitudes needs to be preserved, we multiplied both signals by $\frac{1}{A_1}$. By changing only the amplitudes in (1) and (2), input signals are:

$$Sin = k \sin(\theta), \quad (6)$$
$$Cos = \cos(\theta), \quad (7)$$

where k represents $\frac{B_1}{A_1}$.

By varying the parameter k from 0 to infinity, it was found that, the error specter consists of even harmonics only. It was also observed that phase shift didn't change. When k approaches infinity, the amplitude of harmonics

approaches $\frac{180}{\pi}\frac{2}{n}$, where n represents n-th harmonic. Eq. (8) which contains even harmonics only.

$$\varepsilon(k \to \infty) = \frac{180}{\pi} \sum_{n=1}^{\infty} \frac{1}{n} \sin 2n\theta \qquad (8)$$

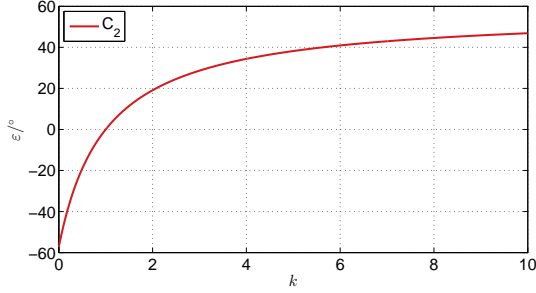Because second harmonic is the largest, we approximated it first (Figure 1).

Figure 1: Waveform of the second harmonic depending on k

Best approximation was rational function (9), with summed squared error (SSE) $1.18 \cdot 10^{-10}$ degrees.

$$C_2(k) = \frac{180}{\pi} \cdot \frac{k-1}{k+1} \qquad (9)$$

It was assumed, that higher order harmonics were correlated with base harmonic. Function, that describes error depending on k is presented in Fourier series form (10).

$$\varepsilon(k) = \frac{180}{\pi} \sum_{n=1}^{\infty} \frac{1}{n}\left(\frac{k-1}{k+1}\right)^n \sin 2n\theta \qquad (10)$$

By replacing k with ratio of amplitudes $\frac{B_1}{A_1}$, we get final equation

$$\varepsilon(A_1, B_1) = \frac{180}{\pi} \sum_{n=1}^{\infty} \frac{1}{n}\left(\frac{B_1 - A_1}{B_1 + A_1}\right)^n \sin 2n\theta, \quad (11)$$

which is valid for positive ratio of amplitudes only.

$$\frac{B_1}{A_1} \geq 0.$$

2.2 Defining of error at non-orthogonality

In second case, it was examined the impact of phase deformation. Input signals are represented as:

$$Sin = \sin(\theta + \varphi_s) \qquad (12)$$
$$Cos = \cos(\theta + \varphi_c) \qquad (13)$$

Error was analyzed for φ_s and φ_c individually, in the end equations were combined.

Worst case of error is, when φ_s approaches $90°$ and can be presented as Fourier series (14). Error consists of DC component and even harmonics only.

$$\varepsilon(\varphi_s \to 90°) = 45° - \frac{180}{\pi} \sum_{n=1}^{\infty} \frac{1}{n} \sin(2n\theta) \qquad (14)$$

Correlation between amplitudes and φ_s yields tangent function (Figure 2). DC component and phase of error were being changed linearly. Tangent function approximate second harmonic with SSE of $1.18 \cdot 10^{-10}$ degrees.
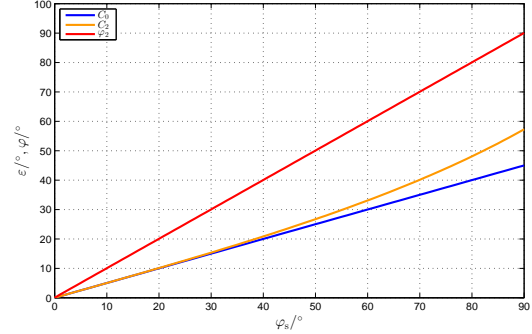

Figure 2: Waveforms of DC component C_0, amplitude of second harmonic C_2 and phase of second harmonic φ_2 compared to ideal cosine signal, due to phase shift φ_s

Same procedure be applied for parameter φ_c as well. Because error from (12) and (13) is independent, their contribution can be combined into (15).

$$\varepsilon(\varphi_s, \varphi_c) = \frac{\varphi_s + \varphi_c}{2} +$$
$$\frac{180}{\pi} \sum_{n=1}^{\infty} \frac{1}{n}\left(\tan\frac{\varphi_s - \varphi_c}{2}\right)^n \sin(2n\theta + n(90° + \varphi_s + \varphi_c))$$
$$(15)$$

Expression (15) is valid only for range:

$$\varphi_s - \varphi_c \in [-90°, 90°]$$

2.3 Defining of error for DC component in one input signal only

By varying DC component in (1) and (2) equations are:
$$Sin = \sin(\theta) + B_0 \qquad (16)$$
$$Cos = \cos(\theta) + A_0. \qquad (17)$$

When parameter A_0 approaches infinity, error is described by eq. (18).

$$\varepsilon(A_0 \to \infty) = \frac{180}{\pi} \sum_{n=1}^{\infty} \frac{2}{n} \sin(n\theta + n180°). \qquad (18)$$

Error does not contain DC component and with the first harmonic being the highest. The waveform from figure 3, was split into 3 parts based on ratio between offset and amplitude. Expression which best approximate waveform of first harmonic of error with SSE of $1.21 \cdot 10^{-7}$ degrees is in exponential and linear form (19):

$$\varepsilon(A_0, A_1) =$$
$$\begin{cases} \frac{180}{\pi} \sum_{n=1}^{\infty} \frac{1}{n}(2 - |\frac{A_0}{A_1}|^{-n}) \sin(n\theta), & \frac{A_0}{A_1} \leq -1 \\ \frac{180}{\pi} \sum_{n=1}^{\infty} (-1)^n \frac{1}{n}(\frac{A_0}{A_1})^n \sin(n\theta), & |\frac{A_0}{A_1}| \leq 1 \\ \frac{180}{\pi} \sum_{n=1}^{\infty} (-1)^n \frac{1}{n}(2 - (\frac{A_0}{A_1})^{-n}) \sin(n\theta), & \frac{A_0}{A_1} \geq 1 \end{cases}$$
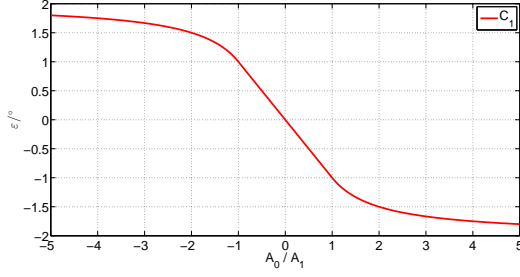$$(19)$$

Figure 3: Waveform of amplitude of first harmonic depending on $\frac{A_0}{A_1}$

Same procedure be applied for parameter B_0 as well. Result is eq. (20).

$$\varepsilon(B_0, B_1) =$$
$$\begin{cases} \frac{180}{\pi} \sum_{n=1}^{\infty} \frac{1}{n}(2 - |\frac{B_0}{B_1}|^{-n})\sin(n\theta - 90°n), & \frac{B_0}{B_1} \leq -1 \\ \frac{180}{\pi} \sum_{n=1}^{\infty} \frac{1}{n}(\frac{B_0}{B_1})^n \sin(n\theta + 90°n), & |\frac{B_0}{B_1}| \leq 1 \\ \frac{180}{\pi} \sum_{n=1}^{\infty} \frac{1}{n}(2 - (\frac{B_0}{B_1})^{-n})\sin(n\theta° + 90n), & \frac{B_0}{B_1} \geq 1 \end{cases}$$
$$(20)$$

2.4 Defining of error for same DC component in both input signals

Input signals can also contain same DC component. This happen to resolver signals acquired at improper installation of stator coils. Same analysis as in 2.3 was made and result is presented in eq. (21).

$$\varepsilon(A_0, B_0 = A_0, A_1) =$$
$$\begin{cases} \frac{180}{\pi} \sum_{n=1}^{\infty} \frac{1}{n}(2 - |\sqrt{2}\frac{A_0}{A_1}|^{-n})\sin(n\theta - 45°n), & \frac{A_0}{A_1} \leq -\frac{\sqrt{2}}{2} \\ \frac{180}{\pi} \sum_{n=1}^{\infty} \frac{1}{n}(\sqrt{2}\frac{A_0}{A_1})^n \sin(n\theta + 135°n), & |\frac{A_0}{A_1}| \leq \frac{\sqrt{2}}{2} \\ \frac{180}{\pi} \sum_{n=1}^{\infty} \frac{1}{n}(2 - (\sqrt{2}\frac{A_0}{A_1})^{-n})\sin(n\theta + 135°n), & \frac{A_0}{A_1} \geq \frac{\sqrt{2}}{2} \end{cases}$$
$$(21)$$

2.5 Impact of CCM signal to error

CCM signal can be acquired at improper installation of rotor part of resolver. Added common mode signal to input signals was analyzed for each parameter individually. This paper presents procedure for CCM of cosine signal only. Result of CCM sinusoidal form is appended. Procedure to achieve result was the same.

Procedure started by limitation of error of Δ_c to infinity. CCM effects to amplitudes and phases of input signals, so was expected that error will contain DC component and even harmonics only. Error when Δ_c approaching infinity can be represented in Fourier series form (22).

$$\varepsilon(\Delta_c \to \infty) = 45° - \frac{180}{\pi} \sum_{n=1}^{\infty} \frac{1}{n}\sin(2n\theta). \quad (22)$$

By varying Δ_c and analyzing error specter, none result was found. Than error specter was split to sine and cosine part. In that case waveform of amplitude of second harmonic of error was presented as:

$$C_{2s}(\Delta_c) \cdot \sin(2\theta) + C_{2c}(\Delta_c) \cdot \cos(2\theta) \quad (23)$$

Figure 4 represents waveforms of DC component and split waveform of second harmonic of error.
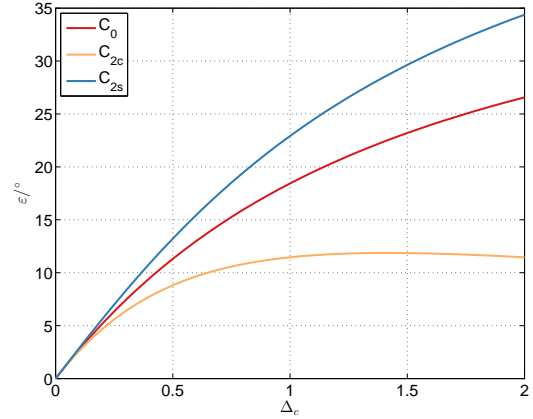

Figure 4: The course of offset and amplitude of second harmonic of error due to Δ_c

DC component was approximated with SSE of $1.94 \cdot 10^{-22}$ degrees with atan function. Waveform of C_{2s} and C_{2c} ware approximated with SSE less then $1.15 \cdot 10^{-9}$ degrees. Functions were merged to function, that represent course of amplitude as $\sqrt{C_{2s}^2 + C_{2c}^2}$ and course of phase as $atan\frac{C_{2c}}{C_{2s}}$. It was assumed, that higher order harmonics were correlated with base harmonic. Final function that described error depending on Δ_c is presented in Fourier series form (24).

$$\varepsilon(A_1, \Delta_c) = atan\frac{\Delta_c}{\Delta_c + 2A_1} +$$
$$+ \frac{180}{\pi} \sum_{n=1}^{\infty} \frac{1}{n}(\frac{\Delta_c}{\sqrt{\Delta_c^2 + 2A_1\Delta_c + 2A_1}})^n$$
$$\sin(2n\theta + n(90° + atan(\frac{\Delta_c + A_1}{A_1}))) \quad (24)$$

Same procedure was made for Δ_s. Result is in eq. (25)

$$\varepsilon(A_1, \Delta_s) = -atan\frac{\Delta_s}{\Delta_s + 2A_1} +$$
$$+ \frac{180}{\pi} \sum_{n=1}^{\infty} \frac{1}{n}(\frac{\Delta_s}{\sqrt{\Delta_s^2 + 2A_1\Delta_s + 2A_1}})^n$$
$$\sin(2n\theta + n(90° - atan(\frac{\Delta_s + A_1}{A_1}))) \quad (25)$$

Eq. (24) and (25) are valid for only:

$$\Delta_s, \Delta_c > -A_1$$

3 Comment on results

After defining error due to deformation parameter in input signal, a fault of approximation (5) was made. Approximated functions were defined with infinite series, during analysis of fault were used first 15 components only. In example input signals have amplitudes $A_1 = 1$

and $B_1 = 1.1$. Difference between error calculated with (11) and error from (5) is presented in figure 5. Fault of approximation is in the vicinity of a numeric error. Comparing errors in frequency specter, showed minimum deviations between harmonics of same frequency.

It is necessary to mention that despite the derivation, the presented types of errors of individual deformations still depends on each other.
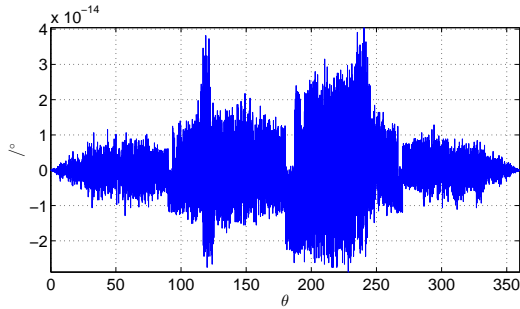

Figure 5: Difference between predicted (11) and actual error

4   Conclusion

With methods described in this paper, improper installation of encoders and resolvers can be uncovered from analyzing error only. Content of higher harmonics in error become non-negligible at major mismatches. This paper presents impact of signal mismatch, non-orthogonality, DC offset and common mode signal to output error of atan2 function.

Input signals can include higher harmonics distortion, which is not described in this paper. The impact of distortion of the input signals in the atan2 function to the output error offers many challenges for further work.

References

[1] Gachter J., Hirz M.,Seebacher R., "Impact of Rotor Position Sensor Errors on Speed Controlled Permanent Magnetized Synchronous Machines", IEEE 12th International Conference on Power Electronics and Drive Systems (PEDS), pp.822-830, 12-15 Dec. 2017

[2] Brugnano F., Concari C., Imamovic E., Savi F., Toscani A., Zanichelli R., "A simple and accurate algorithm for speed measurement in electric drives using incremental encoder", IECON 2017 - 43rd Annual Conference of the IEEE Industrial Electronics Society, pp. 8551-8556, 29 Oct.-1 Nov. 2017

[3] Reddy B.P., Murali A., Shaga G., "Low Cost Planar Coil Structure for Inductive Sensors to Measure Absolute Angular Position", 2017 2nd International Conference on Frontiers of Sensors Technologies (ICFST), pp.14-18, 14-16 April 2017

[4] Zhang Z., Ni F., Liu H., Jin M., "Theory analysis of a new absolute position sensor based on electromagnetism", International Conference on Automatic Control and Artificial Intelligence, pp.2204-208, 3-5 Mar. 2012

[5] Lara J., Chandra A., "Position Error Compensation in Quadrature Analog Magnetic Encoders through an Iterative Optimization Algorithm", IECON 2014 - 40th Annual Conference of the IEEE Industrial Electronics Society, pp.3043-3048, 29 Oct.-1 Nov. 2014

[6] Qi Lin, T. Li, Z. Zhou, "Error Analysis and Compensation of the Orthogonal Magnetic Encoder", Proceedings of IEEE ICMCC Conference, pp.11-14, 21-23 Oct. 2011

[7] Hanselman D.C., "Resolver Signal Requirements for High Accuracy Resolver-to-Digital Conversion", IEEE Transactions on Industrial Electronics, vol.37, no.6, pp.556-561, Dec. 1990

[8] Demierre M., "Improvements of CMOS Hall Microsystems and Application for Absolute Angular Position Measurements", PhD. thesis, pp. 152-161, Federal Polytechnic School of Lausanne, Switzerland, 2003